Noninvasive determination of cell nucleoplasmic viscosity by fluorescence correlation spectroscopy

Lifang Liang*
Xichao Wang*
Da Xing
Tongsheng Chen
South China Normal University
Ministry of Education
Key Laboratory of Laser Life Science & Institute of Laser Life Science
Guangzhou 510631, China

Wei R. Chen
South China Normal University
Ministry of Education
Key Laboratory of Laser Life Science & Institute of Laser Life Science
Guangzhou 510631, China
and
University of Central Oklahoma
Department of Engineering and Physics
College of Mathematics and Science
Edmond, Oklahoma 73034

Abstract. Noninvasive and reliable quantification of rheological characteristics in the nucleus is extremely useful for fundamental research and practical applications in medicine and biology. This study examines the use of fluorescence correlation spectroscopy (FCS) to noninvasively determine nucleoplasmic viscosity (η_{nu}), an important parameter of nucleoplasmic rheology. Our FCS analyses show that η_{nu} of lung adenocarcinoma (ASTC-a-1) and HeLa cells are 1.77 ± 0.42 cP and 1.40 ± 0.27 cP, respectively, about three to four times larger than the water viscosity at 37 °C. η_{nu} was reduced by 31 to 36% upon hypotonic exposure and increased by 28 to 52% from 37 to 24 °C. In addition, we found that η_{nu} of HeLa cells reached the lowest value in the S phase and that there was no significant difference of η_{nu} between in the G1 and G2 phases. Last, nucleoplasmic viscosity was found to be larger than cytoplasmic viscosity in both HeLa and ASTC-a-1 cells. These results indicate that FCS can be used as a noninvasive tool to investigate the microenvironment of living cells. This is the first report on the measurement of η_{nu} in living cells synchronized in the G1, S, and G2 phases. [DOI: 10.1117/1.3088141]

Keywords: fluorescence correlation spectroscopy (FCS); nucleoplasmic viscosity; cytoplasmic viscosity; cell synchronization; nucleoplasmic rheology.

Paper 07475RRRR received Nov. 29, 2007; revised manuscript received Dec. 30, 2008; accepted for publication Jan. 14, 2009; published online Mar. 19, 2009.

1 Introduction

Nucleoplasmic rheology has become a subject of growing interest in the field of nanomedicine, which applies nanoscale devices to repairing genetic defects, delivering therapeutic agents, detecting viruses, and killing cancer cells at the molecular level.[1,2] Designing these nanoscale devices is commonly based on biomolecules such as DNA, RNA polymerase, and DNA helicase in the nucleoplasm.[3,4] Knowledge of nucleoplasmic rheology can help clarify the dynamics of intranuclear molecules, thereby advancing nanomedicine. This study focuses on nucleoplasmic viscosity, one of the important parameters that quantify rheological characteristics in the nucleus. Nucleoplasmic viscosity produces friction forces that must be overcome by intranuclear molecules. Its effect on the motion of molecules should be taken into account especially when designing motors for nanorobots.[5]

Several traditional methods exist for the measurement of nucleoplasmic viscosity.[6–9] However, they have limitations such as photodamage of living cells, relatively low resolution, and strict requirements. Invasion is a serious problem in living cell measurement, since it can lead to a deviation from normal levels of nucleoplasmic viscosity. Thus, there remains a need for reliable and noninvasive techniques to measure nucleoplasmic viscosity in living cells.

Fluorescence correlation spectroscopy (FCS) is particularly attractive for this application. First introduced by Magde et al., FCS is a single-molecule technique that has been widely used in biological research and nanoscale science.[10–16] Through a time correlation analysis of spontaneous intensity fluctuations, this technique with enhanced green fluorescence protein (EGFP) as a probe is capable of determining fluid viscosity according to the Stokes-Einstein equation.[17] FCS has several advantages over traditional methods. The most attractive advantage is its noninvasive nature. Low laser intensity (10^{-4} to 10^{-6} W) does not lead to significant photobleaching in FCS.[18] Other methods, such as fluorescence recovery after photobleaching (FRAP), require high laser intensity (up to 200 to 500 mW), which produces free radicals and photodamage to living cells.[19] A second advantage of FCS is its high temporal resolution; it is capable of monitoring very fast processes on the nanosecond scale compared with FRAP, which operates on the millisecond scale. A third advantage of FCS is its relative convenience of measurement; it works even on the nanomolar scale, about 5% of that in FRAP measurement. In addition, fluorescence anisotropy (FA) measurement is limited to fluorescent objects with excited-state lifetimes comparable to their rotational correlation time, whereas FCS has no such requirement.[12] In summary, FCS is a noninvasive

*These authors contributed equally to this work.
Address all correspondence to: Da Xing, Ph.D., Professor, MOE Key Laboratory of Laser Life Science & Institute of Laser Life Science, South China Normal University, Guangzhou 510631, China. Tel.: (+86-20) 8521-0089; Fax: (+86-20) 8521-6052; Email: xingda@scnu.edu.cn.

1083-3668/2009/14(2)/024013/9/$25.00 © 2009 SPIE

tool of high temporal resolution for convenient measurements in living cells.

Previous investigations have focused on nucleoplasmic viscosity of asynchronized cells. It is uncertain whether there are differences in nucleoplasmic viscosity among the G1, S, and G2 phases. This is an important issue because it relates to molecular mechanisms during the cell cycle. In this study, we examined the use of FCS with EGFP as a probe to determine the nucleoplasmic viscosity of living cells. Moreover, we investigated the nucleoplasmic viscosity of cells synchronized in the G1, S, and G2 phases. We verified the qualitative relationship of the nucleoplasmic viscosity and cytoplasmic viscosity in both HeLa and ASTC-a-1 cells, which should be beneficial to the dynamic analysis of nucleocytoplasmic transport.

2 Materials and Methods

2.1 *Cell Culture, Transient Expressions and Synchronization*

Human epithelial carcinoma cells (HeLa) and human lung adenocarcinoma cells (ASTC-a-1) were cultured at 37 °C in Dulbecco's modified Eagle's medium (DMEM, Invitrogen Company, Carlsbad, California) supplemented with 10% fetal calf serum and antibiotics. Cells were seeded into a 20-mm coverslip-bottomed small chamber before all measurements. Transfections of HeLa and ASTC-a-1 cells were carried out by Lipofectamine2000 reagent (Invitrogen Company, Carlsbad, California) with EGFP plasmid (Clontech, Heidelberg, Germany) according to the manufacturer's instructions. The following procedures were used to arrest HeLa cells at specific stages of the cell cycle. Cells enriched in G1 were obtained by treatment with mimosine (Sigma, St. Louis, Missouri Ohio) at 400 μM for 20 h (Refs. 20 and 21). HeLa cells were treated with 2 mM thymidine (Amresco, Solon, Ohio) for 18 to 20 h, thymidine-free media for 9 to 10 h, and additionally with 2 mM thymidine for 18 to 20 h to arrest the cell cycle at the G1/S boundary.[22,23] Then cells were washed twice with PBS and released into the S phase by incubation in fresh normal media again for 4 h, during which the measurement was performed. Cultures with a high percentage of cells in the G2 phase (95%) were obtained by incubating monolayer cultures at the S phase with colchicine (0.04 μg/mL) between 6 and 8 h after removing the second thymidine block.[24] Ultrapure water (18.2 MΩ-cm, ELGA, High Wycombe, Bucks, England) was added into 300 mOsm/L PBS to achieve hypoosmotic (30 mOsm/L) testing solutions. Cells were exposed to osmotic challenge for 5 to 15 min before testing.

2.2 *Preparations for Aqueous Solution with EGFP*

EGFP-expressing and nontransfected cells grown in 50 mL (25 cm^2) culture flasks were washed three times with ice-cold PBS, added to ice-cold 200 μL buffer (50 mM TrisHCl pH 8.0, 150 mM NaCl, 1% Triton X-100, 100 μg/ml PMSF), and then shaken on ice for 30 min. Cells swollen in this buffer were recover into a 1.5 mL Eppendorf tube and then centrifuged for 5 min at 13,200×g. Before measurements, the sample was diluted to 10^{-8} M with ultra-pure water (18.2 MΩ-cm, ELGA, High Wycombe, Bucks, England), and EGFP in aqueous solution was obtained. Glycerin was added into the EGFP aqueous solution to obtain different viscosities: 0.6, 0.7, 1.0, 1.9, 2.9, and 10.1 cP. The pH value of the solution was adjusted to ~7.0.

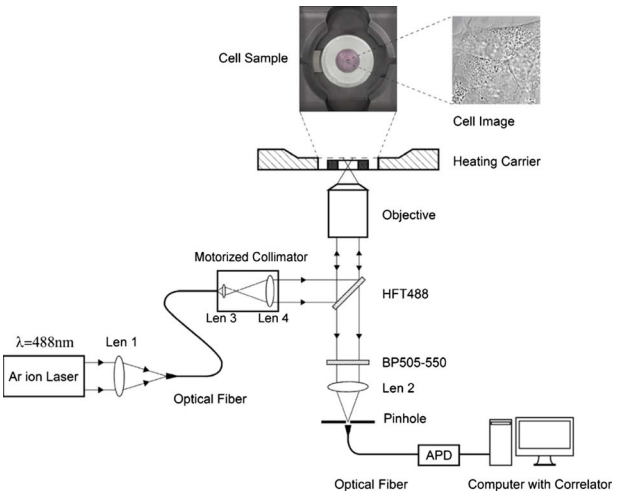

Fig. 1 Schematics of the FCS experimental setup.

2.3 *Instrumentation and Measurement*

Living cell images were acquired by a confocal laser scanning microscope (LSM 510/ConfoCor 2) combination system (Zeiss, Jena, Germany) equipped with a water objective (C-Apochromat 63×/1.2 W corr.). EGFP (the quantum yield is 0.60 and the peak wavelengths of excitation and emission spectrum are 488 nm and 507 to 509 nm, respectively[25]) was excited at 488 nm with an argon-ion laser, and its fluorescence emission was recorded through a 500 to 550-nm IR bandpass filter.

FCS measurements were performed on a ConfoCor2 fluorescence correlation spectrometer (Carl Zeiss, Jena, Germany), which has been described previously.[26,27] The optical path is shown schematically in Fig. 1. Samples were placed on the stage of the inverted microscope. In our experiments, the 488-nm line from an argon-ion laser was used to excite Rhodamine 6G dye or EGFP. The excitation light was reflected by the main dichroic beamsplitter (HFT488) and focused on the focal plane within the sample by an objective (C-Apochromat 63×/1.2 W corr.). The emitted fluorescence via the objective was transmitted through the splitter HFT488. Residual laser excitation light and Raman scattered light were removed by an additional bandpass filter (BP505-550), and photon counts were focused on actively quenched avalanche photodiodes (APD, EG&G, Norfolk County, Massachusetts). A computer station was used to control the instrument and calculate the autocorrelation data of the photoelectron pulses.

The Rhodamine 6G–water solution was measured at room temperature for calibration. In addition, the EGFP aqueous solution and cell samples were placed in the heating carrier of the microscope (CTI-Controller 3700, Carl Zeiss, Germany), which controls the temperature and provides an environment of saturated humidity and 5% CO_2. Aqueous solution measurements were conducted at 30 °C and living cell measurements at 37 °C. All FCS measurements in living cells were

performed after LSM images of a cell were taken, following the protocol as described previously.[28] The z position of the LSM images was determined by adjusting the focusing drive of the microscope when the cross section of the scanned fluorescent cell became the largest. Three types of images were obtained at the same time: fluorescent image, bright-field image, and merged image. Positions in the nucleoplasm were chosen in these LSM images of a cell. Particularly in weakly fluorescent cells, bright-field and merged images made it easy to discriminate the nucleolus from the nucleoplasm and to choose the positions in the nucleoplasm. In order to keep the same height of focus above the coverslip, different positions of a cell were chosen at the same z position, and cells with similar size were chosen in the comparative measurements. In order to avoid photodamaging the cells, the laser intensity from the objective varied from 5 to 12.5 μW during measurements. Autocorrelation curves from the solution were averaged for five successive 60-s-long measurements, and those from living cells were averaged for five successive 30-s-long measurements. To minimize the cell-to-cell variability and to provide valid statistical analysis, we measured sufficient number of cells (more then 40 cells for each phase of cell cycle) grown in different dishes on different days.

2.4 *FCS Analysis*

In an FCS measurement, $\delta F(t)$ of the fluorescence around the average $\langle F(t)\rangle$ due to any dynamic process can be characterized by a normalized autocorrelation function (ACF):

$$G(\tau)=\frac{\langle F(t)F(t+\tau)\rangle}{\langle F(t)\rangle^2}=1+\frac{\langle \delta F(t)\,\delta F(t+\tau)\rangle}{\langle F(t)\rangle^2}. \quad (1)$$

The following fitting formula is the standard expression for the 3-D two-component diffusion model:

$$G(\tau)=1+\frac{1-F+Fe^{-\tau/\tau_{trip}}}{1-F}\times\frac{1}{N}\left\{(1-Y)\frac{1}{\left(1+\frac{\tau}{\tau_{D1}}\right)\left[1+\frac{\tau}{\tau_{D1}}\left(\frac{r_0}{z_0}\right)^2\right]^{1/2}}+Y\frac{1}{\left(1+\frac{\tau}{\tau_{D2}}\right)\left[1+\frac{\tau}{\tau_{D2}}\left(\frac{r_0}{z_0}\right)^2\right]^{1/2}}\right\}, \quad (2)$$

where F denotes the triplet fraction of fluorescent dyes or the average fraction of molecules in the nonfluorescent state,[29] τ_{trip} is the relaxation time of the respective preceeding fraction, $\tau_{Di,i=1,2}$ refers to the characteristic diffusion time during which the i'th species molecule stays in the excitation volume with an axial z_0 to lateral r_0 dimension ratio (namely, the structure parameter $S=z_0/r_0$), N is the mean number of molecules in the excitation volume, and Y is the fraction of the second species. Equation (2) becomes a one-component diffusion model as $Y=0$. The relationship between the diffusion coefficient D_i and the lateral dimension r_0 can be described as;[30]

$$Di=\frac{r_0^2}{4\tau_{Di}}. \quad (3)$$

S and τ_{Di} are determined by fitting the diffusion of free Rhodamine 6G to Eq. (2) with $Y=0$. Assuming that the diffusion coefficient D for Rhodamine 6G in water is 4.22×10^{-10} m^2/s at 20 °C (Refs. 31–33), r_0 was obtained in our calibration measurement as 0.18 μm.

The viscosity of fluids can be calculated according to the Stokes-Einstein equation:

$$D=\frac{kT}{6\pi\eta r}, \quad (4)$$

$$r=\left(\frac{3\cdot m}{4\pi N_A\rho}\right)^{1/3}, \quad (5)$$

where k is the Boltzmann constant, T is the absolute temperature, η is the solvent viscosity, r is the hydrodynamic radius of the molecule, m is the molecular weight, N_A is the Avogadro constant, and ρ is the mean density of the molecule.

Molecular weight and mean density for EGFP are 27 kDa and 1.2 g/cm^3, respectively,[34] and hydrodynamic radius $r=2.1\times10^{-9}$ m is acquired according to Eq. (5). As a result, the viscosity of fluids can be obtained using the diffusion time of EGFP by FCS and by Eq. (3) and Eq. (4).

The influence of EGFP protonation had been taken into account when using Eq. (2), the correction part of which, $(1-F+Fe^{-\tau/\tau_{trip}})/(1-F)$, describes the influence of protonation below pH 8.0 as pointed out by the authors of the previous study.[29]

2.5 *Statistical Analysis*

The statistical significance of differences between groups was evaluated by Student's t-test using SPSS version 13.0 software. Differences were considered as statistically significant at $P<0.05$. All statistical tests were two-sided.

3 Results

3.1 *FCS Analysis of EGFP Diffusion in Aqueous Solution*

The first step undertaken in this study was the analysis of the EGFP diffusion in aqueous solution with various viscosities using FCS. This investigation helps to establish the practical use of FCS in measuring nucleoplasmic viscosity. Figure 2(a) shows the normalized autocorrelation curves of EGFP-expressing cells in an aqueous solution and nontransfected cells as control at 30 °C. The former fits well to the one-component diffusion model by Eq. (2), while the latter does not show any correlation to autofluorescence. This finding indicates that the EGFP gene is normally expressed in the cell. We found that the diffusion coefficient D of EGFP in aqueous solution was 203 ± 7 μm^2/s at 30 °C with a relative standard deviation (RSD) of about 3.5%. Previous study using FRAP showed that the D value of EGFP in PBS solution is 87 ± 11 μm^2/s at room temperature with an RSD of about 13% (Ref. 35), and it can be calculated as 113 ± 14 μm^2/s at 30 °C in terms of the classical Stokes-Einstein relation [Eq. (4)]. Therefore, the smaller RSD value of our result indicates

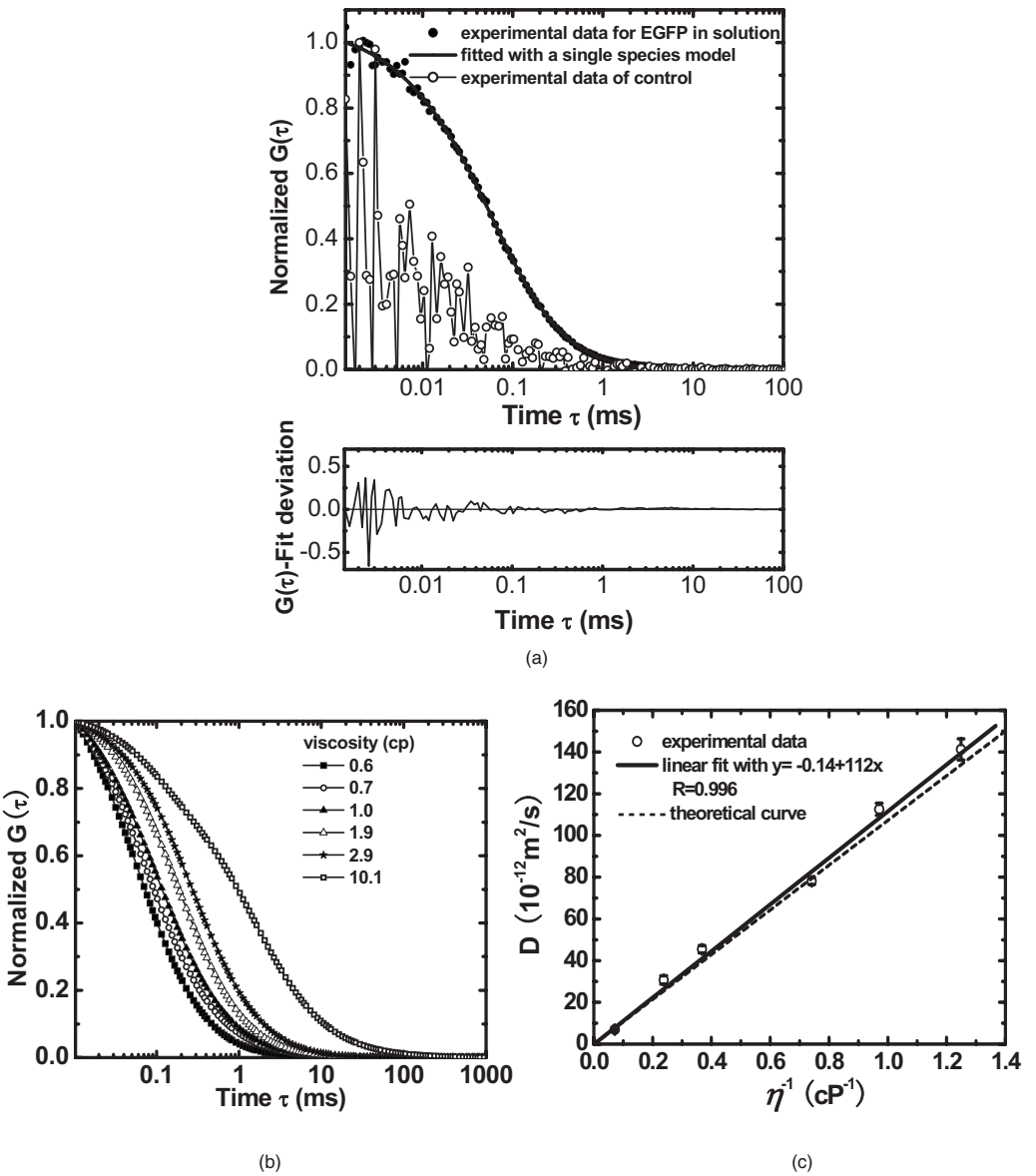

Fig. 2 FCS measurements of EGFP diffusion in aqueous solution. (a) Normalized autocorrelation curves of EGFP-expressing cells and of nontransfected cells in aqueous solution. The autocorrelation curve (●) of EGFP solution fits well to the one-component model (—○–). The autocorrelation curve (—○—) of the solution of nontransfected cells does not show any correlation. (b) Normalized autocorrelation curves of EGFP-glycerin solution with various viscosities: 0.6 (—■—), 0.7 (—○—), 1.0 (—▲—), 1.9 (—△—), 2.9 (—★—), and 10.1 cP (—□—) at 30 °C. (c) The diffusion coefficient for EGFP in glycerin solutions of different viscosities at 30 °C. The line (—) shows that the experimental data fit well to a linear function $y=-0.14+112\times$ with $R=0.996$, compared with the theoretical equation $D=155\eta^{-1}$ (---) at 30 °C.

the stability of this method. In addition, the deviation of the mean D in our measurements from the previous value likely results from different sample compositions due to different methods of solution preparation.

According to Eq. (4), the D value of EGFP is linearly proportional to the reciprocal of viscosity η at the same temperature ($D=155\ \eta^{-1}$ at 30 °C). Therefore, the D value of EGFP in glycerin solution with various viscosities was measured at 30 °C to determine whether our measurement was consistent with the principle discussed earlier. Figure 2(b) presents the normalized autocorrelation curves of EGFP in glycerin solution. D is plotted as a function of η^{-1}, and the experimental data fit the linear function $y=-0.14+112x$ ($R=0.996$), as shown in Fig. 2(c). There is a minor deviation in slope from the expected result of $D=155\ \eta^{-1}$. This discrepancy may be due to the fact that EGFP is not an ideal sphere with a fixed radius, whereas the EGFP protein is often considered to be an ideal sphere for model simplification.[28] The D values and corresponding RSD of EGFP in glycerin solution with different viscosities are summarized in Table 1. The results show that a smaller diffusion coefficient of detected molecules corresponds to a larger RSD, which is consistent with Koppel's theory.[36] Taken together, the analysis of EGFP mobility in aqueous solution indicates that FCS is able to determine fluid viscosity.

Table 1 Diffusion coefficients of EGFP in glycerin solution of different viscosities and the corresponding RSDs (T=30 °C). Data are mean±S.D.

Viscosity (cP)	0.6	0.7	1.0	1.9	2.9	10.1
D ($\mu m^2/s$) mean±S.D.	203±7	163±4	112.5±2.3	65.5±2.6	44.2±2.9	10.0±1.1
RSD	3.55%	2.65%	3.32%	3.96%	6.52%	11.1%

3.2 *Nucleoplasmic Viscosity of Living Interphase Cells*

3.2.1 *FCS analysis of nucleoplasmic viscosity of living HeLa and ASTC-a-1 cells*

Previous studies have suggested that small molecules can diffuse freely and rapidly in the nucleoplasm.[28,37–39] Seksek et al. found that the diffusion coefficient D of small molecules (<500 kDa) in cells relative to that in water (D/D_0) was independent of their size.[37] Pack et al. also found no significant difference by FCS for D/D_0 of $EGFP_{n=2,3,4,5}$ ($EGFP_2$ to $EGFP_5$: different levels of oligomeric EGFP with molecular weights of 60, 90, 120, and 150 kDa, respectively).[28] These results show that molecules with a molecular mass (<500 kDa) can diffuse freely in the nucleoplasm. EGFP is a 27 kDa-protein without specific biological function in living cells. Moreover, Guigas et al. recently have reported that GFP showed normal diffusion in nucleoplasm and cytoplasm because the anomality of GFP was found to be about 1 in the two compartments using the anomalous diffusion model.[40] Therefore, we used EGFP as a probe and applied the free diffusion model in FCS analysis of nucleoplasmic viscosity.

Weakly fluorescent cells were selected in order to satisfy the requirement of nanomolar concentration in FCS measurement. η_{nu} of each cell was the average of data from several randomly selected positions in the nucleus. In our experiments, most of the autocorrelation curves from EGFP-expressing cells fit well to the one-component diffusion model, while autofluorescence from nontransfected cells did not show any correlation, as shown in Fig. 3. This result further suggests that the transport of EGFP is purely Brownian in the nucleus, as is expected.[41,42] In a few of our experiments, the two-component model provided better fits to the autocorrelation function, as reported by some previous studies.[28] These findings indicate that the nucleus contains regions where EGFP molecules diffuse with different mobilities. This is because there are some subcellular organelles such as nucleoskeleton or some fixed nuclear compartments,[28,38,43] which trap some EGFP molecules and make them stay longer in the excited volume.[44] Only the fast fraction of EGFP molecules that are not trapped by subcellular organelles can freely diffuse in nucleoplasm. In the case of the two-component model, we chose the diffusion time only from the fast fraction to calculate η_{nu}. η_{nu} of HeLa and ASTC-a-1 cells were determined to be 1.40±0.27 cP and 1.77±0.42 cP, respectively, about three to four times as viscous as water at 37 °C. This result is consistent with previous studies using traditional methods.[7,28,37] Photoactivation analysis also suggested that the apparent nucleoplasmic viscosity of normal rat kidney cells was about 3.1 times higher than water viscosity at 37 °C (Ref. 7). In addition, we found that in the two-component model, the average D over fast and slow fractions of HeLa cells was 55±10.8 $\mu m^2/s$ (mean±S.D.), higher than Braga's FRAP result of 33±4 $\mu m^2/s$ (Ref. 45). The reason is possibly that FRAP provides the averaged diffusion coefficient of EGFP, with fast and slow rates diffusing from the outside to the inside of the excited volume. Our results further indicate that the free diffusion model is suited for the FCS analysis of nucleoplasmic viscosity and that FCS measurement is reliable.

3.2.2 *Nucleoplasmic viscosity of living cells in different physiological conditions*

To determine whether FCS could be used to detect differences in intracellular fluid viscosity, we measured η_{nu} of living cells under different physiological conditions (Fig. 4). Figure 4(a) displayed the representative autocorrelation curves of a cell at 24 °C and warmed to 37 °C (outset) and of cells exposed to hypotonic media versus normal media (inset). The correlation function obtained at 24 °C showed a broad distribution, and the correlation function obtained in hypotonic media covered a shorter lag time when compared with their respective con-

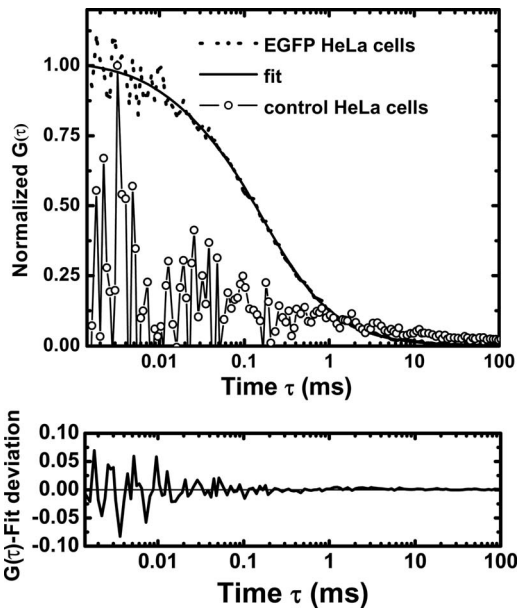

Fig. 3 The normalized autocorrelation curve of EGFP in the nucleoplasm of HeLa cells versus that of nontransfected HeLa cells as control. The data from EGFP-expressing cells (···) fit well to the one-component model (—), while the data from nontransfected cells (—○—) do not show any correlation.

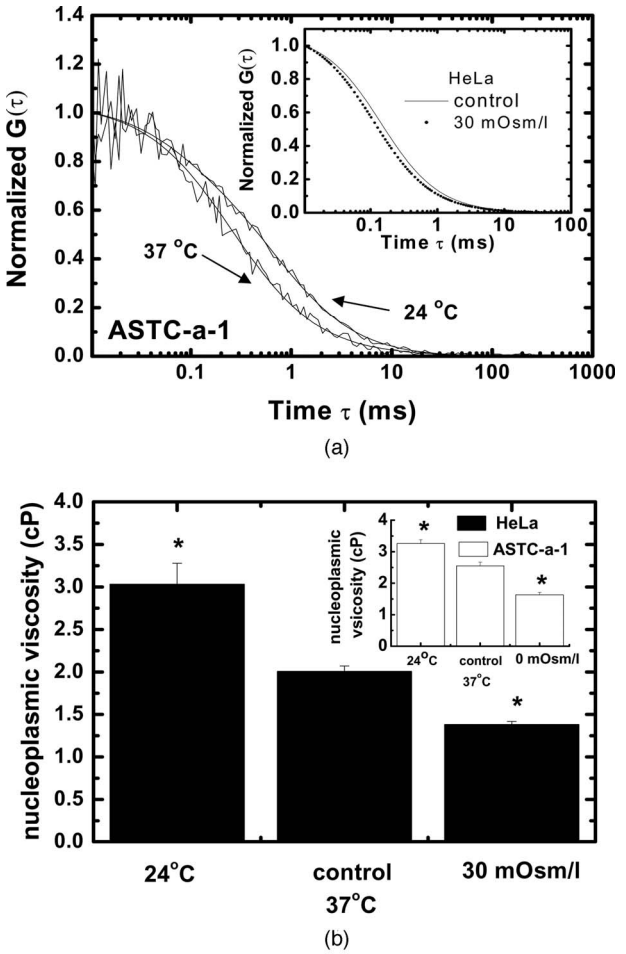

Fig. 4 Nucleoplasmic viscosity of living HeLa and ASTC-a-1 cells in different physiological conditions. (a) Representative normalized autocorrelation curves of EGFP in the nucleoplasm of an ASTC-a-1 cell at 37 °C and cooled to 24 °C; normalized autocorrelation curves of EGFP in the nucleoplasm of HeLa cells in 30 mOsm/L PBS (---) and in normal medium as control (—) (inset). (b) Nucleoplasmic viscosity of HeLa cells in 30 mOsm/L PBS or at low temperature (24 °C) versus that in normal medium at 37 °C as control; nucleoplasmic viscosity of ASTC-a-1 cells in 0 mOsm/L ultrapure water or at low temperature (24 °C) versus that in normal medium at 37 °C as control (inset). Values are mean±S.E.M; (standard error of mean) asterisks (*) indicate a significant difference compared with respective controls ($P < 0.001$).

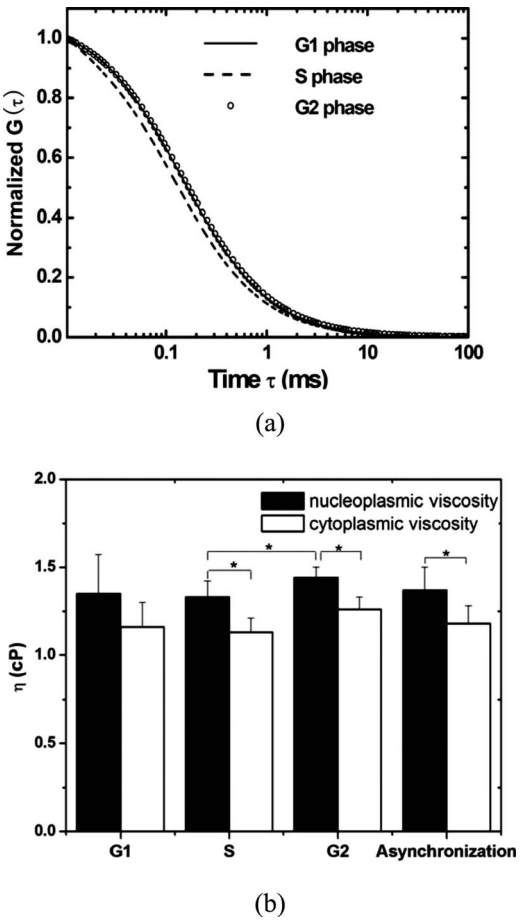

Fig. 5 Nucleoplasmic viscosity of HeLa cells synchronized in the G1, S, and G2 phases. (a) The normalized autocorrelation curves of EGFP in the nucleoplasm of HeLa cells synchronized in the G1 (—), S (···), and G2 phase (○), respectively. (b) Histograms for nucleoplasmic viscosity (η_{nu}) and cytoplasmic viscosity (η_{cyto}) of HeLa cells. G1 phase: 48 cells (nu), 20 cells (cyto); S phase: 61 cells (nu), 22 cells (cyto); G2 phase: 44 cells (nu), 25 cells (cyto); asynchronization: 48 cells (nu), 20 cells (cyto). These data are mean±S.E.M; nu: nucleoplasmic viscosity; cyto: cytoplasmic viscosity. Asterisks (*) indicate statistically significant differences between η_{nu} and η_{cyto} or differences of η_{nu} between the S phase and G1 (G2) phase, $P < 0.05$.

trol groups. Quantitative analysis showed that η_{nu} was reduced by 31 to 36% when cells were exposed to hypotonic media (HeLa: 30 mOsm/l; ASTC-a-1: 0 mOsm/l) and increased by 28 to 52% when cells were cooled from 37 °C to 24 °C [Fig. 4(b)]. The Student's *t*-test using SPSS version 13.0 software also suggested that the η_{nu} of cells in different media was significantly different from that in normal media at 37 °C ($P < 0.001$). These results agree with previous findings.[6,9] Lang et al. found that the nucleoplasmic diffusion coefficient increased by 45 to 85% between 10 and 37 °C through FRAP analysis.[6] Fushimi and Verkman showed that cytoplasmic viscosity of Swiss 3T3 cells increased by ~39% from 32 to 24 °C by FA measurement.[9] Our results indicate that FCS is capable of detecting changes in nucleoplasmic viscosity when cells are under different physiological conditions.

3.2.3 *Nucleoplasmic viscosity of HeLa cells synchronized in the G1, S, and G2 phases*

To investigate the nucleoplasmic viscosity of HeLa cells within the cell cycle, we synchronized HeLa cells in the G1, S, and G2 phases and then measured nucleoplasmic viscosity in each phase. Our results showed that η_{nu} of HeLa cells in the G1, S, and G2 phases were 1.35 ± 0.22 cP (48 cells), 1.33 ± 0.09 cP (61 cells), and 1.44 ± 0.06 cP (44 cells), respectively (mean ± S.D.). η_{nu} in the S phase was about 7.9% smaller than that in the G2 phase. The corresponding autocorrelation curves are shown in Fig. 5(a). Statistical analysis with the Student's *t*-test also suggests that the difference in η_{nu} between the S and G1 phases is statistically significant

($P<0.05$), while the difference between the G1 and G2 phases is not significant ($P>0.05$). We also found a similar qualitative relationship of cytoplasmic viscosity (η_{cyto}) among these three phases [Fig. 5(b); see also Sec. 3.2.4]. Therefore, the viscosity of the aqueous domain in HeLa cells is smallest in the S phase.

The changes of intracellular water relative content and ion concentration within the cell cycle may be the main reason why nucleoplasmic viscosity reduces to its lowest value compared to the G1/G2 phase. It has been shown that permeability to water peaks at the initiation of the S phase and progressively decreases after mitosis and that the volume of cell water is the highest during the S phase and the early G2 phase.[46] The inward current of Cl^- and K^+ was found to be the highest in the early G1 phase and the lowest in the S phase.[47,48] These evidences qualitatively support our results. However, additional efforts should be made in the future to determine whether it is a general conclusion that intracellular fluid viscosity becomes the lowest in the S phase. It is an important subject in cell biology, which will provide a reference to biologists engaging in investigation on cell cycle biology. Our current study demonstrated that FCS was a potentially reliable technique to investigate intracellular fluid viscosity in a specific cell phase or under different physiological conditions.

It is very important to analyze the molecular and cellular changes during different cell cycle transition in foundational biological and medical research fields. For example, telomerase activity has been detected in the vast majority of human tumors, but only in a few normal somatic cells.[49] Its activity is regulated in a cell cycle–dependent manner. Maximum telomerase activity was detected in the S phase, with barely detectable levels observed at the G2/M phase.[50] However, traditional methods of cell cycle analysis would inevitably impair the living cells. The most common cell cycle analysis method, flow cytometry, needs propidium iodide (PI) to stain sample cells. PI intercalates into double-stranded nucleic acids; it is excluded by viable cells but can penetrate cell membranes of dying or dead cells.[51] Therefore, this routine cell cycle analysis method would lead directly to the death of sample cells and certainly affect further mechanism studies on these same sample cells. Primary sample cells derived directly from patients or possible cases are generally difficult to obtain and have not been subcultured for fear of affecting the accurate studies of the tumorigenesis mechanism. In this situation, FCS is capable of resolving the problem. To understand the relationship between functional proteins and the nuclear microenvironment, it is helpful to analyze the mobility of standard protein molecules with well-defined hydrodynamic properties as well as functional nuclear proteins or labeled macromolecules.[52,53] FSC is useful to this kind of study. The characteristics of FCS (fast, accurate, and noninvasive) demonstrated in our study indicate its promising application in biological and medical foundational studies.

3.2.4 *Comparison of nucleoplasmic viscosity and cytoplasmic viscosity*

FCS was applied to compare η_{nu} with η_{cyto} in ASTC-a-1 and HeLa cells. Statistical analysis shows that the average η_{cyto} of ASTC-a-1 cells is 1.63 cP, about 7.9% smaller than η_{nu} (Table 2) and that there are significant differences between η_{nu} and η_{cyto} of G1, S, G2, or asynchronizied HeLa cells [$P<0.05$; Fig. 5(b)]. We also found similar results when comparing η_{cyto} with η_{nu} of the same HeLa cell. Table 2 shows the ratio of η_{nu} to η_{cyto}, 1.1 to 1.2, obtained respectively from single HeLa cells in the G1, S, and G2 phases. As shown in Fig. 6, the lag time of the correlation curve in the nucleoplasm was longer than that in the cytoplasm of the same HeLa cells, indicating that it took EGFP longer to go through the excitation volume in the nucleoplasm. These re-

Table 2 Comparison between nucleoplasmic viscosity and cytoplasmic viscosity of HeLa cells synchronized in the G1, S, and G2 phases and of ASTC-a-1 cells. Data are mean±S.D.

Cell type	Nucleoplasmic viscosity (cP)	Cytoplasmic viscosity (cP)	Viscosity ratio (nucleoplasm to cytoplasm)
G1-HeLa	1.35±0.22 (3 positions)	1.16±0.14 (3 positions)	1.2
S-HeLa	1.33±0.09 (3 positions)	1.13±0.08 (3 positions)	1.2
G2-HeLa	1.44±0.06 (3 positions)	1.26±0.07 (3 positions)	1.1
ASTC-a-1	1.77±0.42 (25 cells)	1.63±0.49 (25 cells)	1.1

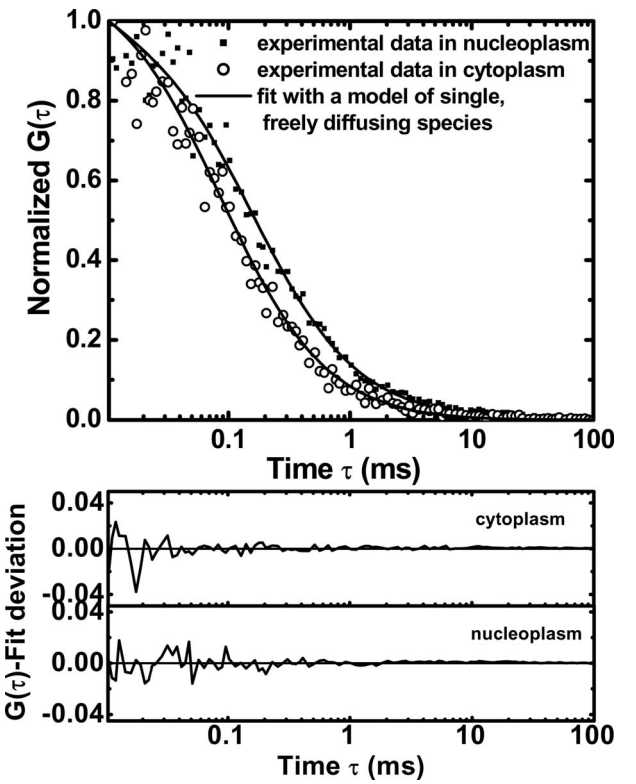

Fig. 6 The normalized autocorrelation curves of EGFP in the nucleoplasm (■) and in the cytoplasm (○) of the same HeLa cell. Both curves fit well to the one-component model (—).

sults demonstrated that nucleoplasmic viscosity is higher than cytoplasmic viscosity.

Guigas et al. recently found that the cytoplasm is more viscoelastic than the nucleoplasm.[40] They showed that nanoprobes diffused anomalously (the anomaly, a, is in the range of 0.5 to 0.6) within the cytoplasm and nucleoplasm because macromolecules crowding greatly hindered their movement, while green fluorescent protein (GFP) with smaller size diffused normally ($a \approx 1$) because the crowding was a less important factor on this scale, consistent with our current work. Therefore, the elastic response subsides and the two compartments appear solely viscose when GFP is used as a probe. In terms of the Guigas et al. finding that cytoplasmic viscoelasticity is higher than nucleoplasmic viscoelasticity, our result ($\eta_{nu} > \eta_{cyto}$) further supports the Guigas et al. conclusion that cytoplasm has a higher degree of macromolecule crowding than nucleus.[40]

4 Conclusion

In this study, FCS was applied to noninvasively determine nucleoplasmic viscosity of living cells. To our best knowledge, this is the first report on nucleoplasmic viscosity of living cells synchronized in the G1, S, and G2 phases.

In living cell measurements, we found that the nucleoplasm of HeLa and ASTC-a-1 cells was three to four times as viscous as water, a finding in agreement with previous results by traditional methods. Moreover, we examined the practical use of FCS in detecting changes of nucleoplasmic viscosity of cells under different physiological conditions such as hypotonic exposure and low temperature. We found that intracellular fluid viscosity reached its minimum during the S phase in HeLa cells. Last, we showed that nucleoplasmic viscosity was higher than cytoplasmic viscosity. It is obvious that these spatiotemporal differences of intracellular fluid viscosity should be taken into account in the dynamic analysis of biomolecules in the cell cycle or nucleocytoplasmic transport.

In summary, this study suggests that FCS can provide a reliable estimation of rheological characteristics in the nucleus and that it is a noninvasive tool to quantify the dynamics of biomolecules *in vivo*, which is useful in applications of nanotechnology to medicine and biology.

Acknowledgments

This research is supported by the National Natural Science Foundation of China (30470494, 30627003, 30670507) and the Natural Science Foundation of Guangdong Province (7117865, F051001).

References

1. C. A. Haberzettl, "Nanomedicine: destination or journey?," *Nanotechnology* **13**, R9–R13 (2002).
2. S. M. Moghimi, A. C. Hunter, and J. C. Murray, "Nanomedicine: current status and future prospects," *FASEB J.* Federation of American Societies for Experimental Biology, **19**, 311–330 (2005).
3. K. Kubik-Bogunia and M. Sugisaka, "From molecular biology to nanotechnology and nanomedine," *BioSystems* **65**, 123–138 (2002).
4. C. M. Niemeyer, "Nanotechnology: tools for the biomolecular engineer," *Science* **297**, 62–63 (2002).
5. A. A. G. Requicha, "Nanorobots, NEMS, and Nanoassembly," *Proc. IEEE* **91**, 1922–1933 (2003).
6. I. Lang, M. Scholz, and R. Peters, "Molecular mobility and nucleocytoplasmic flux in hepatoma cells," *J. Cell Biol.* **102**, 1183–1190 (1986).
7. J. Beaudouin, F. Mora-Bermúdez, T. Klee, N. Daigle, and J. Ellenberg, "Dissecting the contribution of diffusion and interactions to the mobility of nuclear proteins," *Biophys. J.* **90**, 1878–1894 (2006).
8. Y. Tseng, J. S. Lee, T. P. Kole, I. Jiang, and D. Wirtz, "Micro-organization and visco-elasticity of the interphase nucleus revealed by particle nanotracking," *J. Cell. Sci.* **117**, 2159–2167 (2004).
9. K. Fushimi and A. S. Verkman, "Low viscosity in the aqueous domain of cell cytoplasm measured by picosecond polarization microfluorimetry," *J. Cell Biol.* **112**, 719–725 (1991).
10. E. L. Elson and D. Magde, "Fluorescence correlation spectroscopy. 1. Conceptual basis and theory," *Biopolymers* **13**, 1–27 (1974).
11. D. Magde, W. W. Webb, and E. L. Elson, "Thermodynamic fluctuations in a reacting system—measurement by fluorescence correlation spectroscopy," *Phys. Rev. Lett.* **29**, 705–708 (1972).
12. O. Krichevsky and G. Bonnet, "Fluorescence correlation spectroscopy: the technique and its applications." *Rep. Prog. Phys.* **65**, 251–297 (2002).
13. Z. Wang, J. V. Shah, M. W. Berns, and D. W. Cleveland, "*In vivo* quantitative studies of dynamic intracellular processes using fluorescence correlation spectroscopy," *Biophys. J.* **91**, 343–351 (2006).
14. S. A. Tatarkova, A. K. Verma, D. A. Berk, and C. J. Lloyd, "Quantitative fluorescence microscopy of macromolecules in gel and biological tissue," *Phys. Med. Biol.* **50**, 5759–5768 (2005).
15. C. R. Sabanayagam and J. R. Lakowicz, "Fluctuation correlation spectroscopy and photon histogram analysis of light scattered by gold nanospheres," *Nanotechnology* **18**, 335402–335408 (2007).
16. J. M. Moran-Mirabal, A. J. Torres, K. T. Samiee, B. A. Baird, and H. G. Craighead, "Cell investigation of nanostructures: zero-mode waveguides for plasma membrane studies with single molecule resolution," *Nanotechnology* **18**, 195101–195110 (2007).
17. K. M. Berland, P. T. C. So, and E. Gratton, "Two-photon fluorescence correlation spectroscopy: method and application to the intracellular environment," *Biophys. J.* **68**, 694–701 (1995).
18. V. Vukojević, A. Pramanik, T. Yakovleva, R. Rigler, L. Terenius, and G. Bakalkin, "Study of molecular events in cells by fluorescence correlation spectroscopy," *Cell. Mol. Life Sci.* **62**, 535–550 (2005).
19. A. Partikian, B. Ölveczky, R. Swaminathan, Y. Li, and A. S. Verkman, "Rapid diffusion of green fluorescent protein in the mitochondrial matrix," *J. Cell Biol.* **140**, 821–829 (1998).
20. S. A. Didichenko, C. M. Fragoso, and M. Thelen, "Mitotic and stress-induced phosphorylation of HsPI3K-C2a targets the protein for degradation," *J. Biol. Chem.* **278**, 26055–26064 (2003).
21. T. Krude, "Mimosine arrests proliferating human cells before onset of DNA replication in a dose-dependent manner," *Exp. Cell Res.* **247**, 148–159 (1999).
22. T. Taniguchi, I. Garcia-Higuera, P. R. Andreassen, R. C. Gregory, M. Grompe, and A. D. D. Andrea, "S-phase-specific interaction of the Fanconi anemia protein, FANCD2, with BRCA1 and RAD51," *Blood* **100**, 2414–2420 (2000).
23. H. Gao, X. B. Chen, and C. H. McGowan, "Mus81 endonuclease localizes to nucleoli and to regions of DNA damage in human S-phase cells," *Mol. Biol. Cell* **14**, 4826–4834 (2003).
24. A. A. Al-Bader, A. Orengo, and P. N. Rao, "G2 phase-specific proteins of HeLa cells," *Proc. Natl. Acad. Sci. U.S.A.* **75**, 6064–6068 (1978).
25. R. Y. Tsein, "The green fluorescent protein," *Annu. Rev. Biochem.* **67**, 509–544 (1998).
26. R. Rigler, Z. Foldes-Papp, F. J. Meyer-Almes, C. Sammet, M. Volcker, and A. Schnetz, "Fluorescence cross-correlation: a new concept for polymerase chain reaction," *J. Biotechnol.* **63**, 97–109 (1998).
27. K. Saito, I. Wada, M. Tamura, and M. Kinjo, "Direct detection of caspase-3 activation in single live cells by cross-correlation analysis," *Biochem. Biophys. Res. Commun.* **324**, 849–854 (2004).
28. C. Pack, K. Saito, M. Tamura, and M. Kinjo, "Microenvironment and effect of energy depletion in the nucleus analyzed by mobility of multiple oligomeric EGFPs," *Biophys. J.* **91**, 3921–3936 (2006).
29. U. Haupts, S. Maiti, P. Schwille, and W. W. Webb, "Dynamics of fluorescence fluctuations in green fluorescent protein observed by fluorescence correlation spectroscopy," *Proc. Natl. Acad. Sci. U.S.A.* **95**, 13573–13578 (1998).
30. P. Schwille and E. Haustein, "Fluorescence correlation spectroscopy: an introduction to its concepts and applications," http://www.biophysics.org/education/schwille.pdf (2004).
31. K. Weisshart, V. Jungel, and J. S. Briddon, "The LSM 510 META-Confocor 2 system: an integrated imaging and spectroscopic platform

for single-molecule detection," *Curr. Pharm. Biotechnol.* **5**, 135–154 (2004).
32. Z. Petrásek and P. Schwille, "Precise measurement of diffusion coefficients using scanning fluorescence correlation spectroscopy," *Biophys. J.* **94**, 1437–1448 (2008).
33. P.-O. Gendron, F. Avaltroni, and K. J. Wilkinson, "Diffusion coefficient of several rhodamine derivatices as determined by pulsed field gradient—nuclear magetic resonance and fluorescence correlation spectroscopy," *J. Fluoresc.*, **18**, 1093–1101 (2008).
34. C. Zeiss, "Biophysical fundamentals of FCS," Chapter 5 in *Applications Manual LSM 510-Confocor 2 Fluorescence Correlation Spectroscopy*, pp. 62–90, Carl Zeiss Advanced Imaging Microscopy, Germany (2001).
35. R. Swaminathan, C. P. Hoang, and A. S. Verkman, "Photobleaching recovery and anisotropy decay of green fluorescent protein GFP-S65T in solution and cells: cytoplasmic viscosity probed by green fluorescent protein translational and rotational diffusion," *Biophys. J.* **72**, 1900–1907 (1997).
36. D. E. Koppel, "Statistical accuracy in fluorescence correlation spectroscopy," *Phys. Rev. A* **10**, 1938–1945 (1974).
37. O. Seksek, J. Biwersi, and A. S. Verkman, "Translational diffusion of macromolecule-sized solutes in cytoplasm and nucleus," *J. Cell Biol.* **138**, 131–142 (1997).
38. T. Misteli, "Protein dynamics: implications for nuclear architecture and gene expression," *Science* **291**, 843–847 (2001).
39. R. D. Phair and T. Misteli, "High mobility of proteins in the mammalian cell nucleus," *Nature (London)* **404**, 604–609 (2000).
40. G. Guigas, C. Kalla, and M. Weiss, "The degree of macromolecular crowding in the cytoplasm and nucleoplasm of mammalian cells is conserved," *FEBS Lett.* **581**, 5094–5098 (2007).
41. Y. Chen, J. D. Müller, Q. Ruan, and E. Gratton, "Molecular brightness characterization of EGFP *in vivo* by fluorescence fluctuation spectroscopy," *Biophys. J.* **82**, 133–144 (2002).
42. Z. Wang, J. V. Shah, Z. Chen, C. Sun, and M. W. Berns, "Fluorescence correlation spectroscopy investigation of a GFP mutant-enhanced cyan fluorescent protein and its tubulin fusion in living cells with two-photon excitation," *J. Biomed. Opt.* **9**, 395–403 (2004).
43. A. I. Lamond and W. C. Earnshaw, "Structure and function in the nucleus," *Science* **280**, 547–553 (1998).
44. M. Wachsmuth, W. Waldeck, and J. Langowski, "Anomalous diffusion of fluorescent probes inside living cell nuclei investigated by spatially resolved fluorescence correlation spectroscopy," *J. Mol. Biol.* **298**, 677–689 (2000).
45. J. Braga, J. M. P. Desterro, and M. Carmo-Fonseca "Intracellular macromolecular mobility measured by fluorescence recovery after photobleaching with confocal laser scanning microscopes," *Mol. Biol. Cell* **15**, 4749–4760 (2004).
46. A. M. DuPre and H. G. Hempling, "Osmotic properties of Ehrlich ascites tumor cells during the cell cycle," *J. Cell Physiol.* **97**, 381–396 (1978).
47. N. Ullrich and H. Sontheimer, "Cell cycle–dependent expression of a glioma-specific chloride current: proposed link to cytoskeletal changes," *Am. J. Physiol.* **273**, C1290–C1297 (1997).
48. A. Takahashi, H. Yamaguchi, and H. Miyamoto, "Change in K^+ current of HeLa cells with progression of the cell cycle studied by patch-clamp technique," *Am. J. Physiol.* **265**, C328–C336 (1993).
49. H. W. Sharma, J. A. Sokoloski, J. R. Perez, J. Y. Maltese, A. C. Sartorelli, C. A. Stein, G. Nichols, Z. Khaled, N. T. Telang, and R. Narayanan, "Differentiation of immortal cells inhibits telomerase activity," *Proc. Natl. Acad. Sci. U.S.A.* **92**, 12343–12346 (1995).
50. X. Zhu, R. Kumar, M. Mandal, N. Sharma, H. W. Sharma, U. Dhingra, J. A. Sokoloski, R. Hsiao, and R. Narayanan, "Cell cycle–dependent modulation of telomerase activity in tumor cells," *Proc. Natl. Acad. Sci. U.S.A.* **93**, 6091–6095 (1996).
51. A. Kolstad and M. Tuck, "Propidium iodide staining for sub-G1 analysis: hypotonic lysis method," http://www.med.umich.edu/flowcytometry/PDF%20files/HYPOpi.pdf (1999).
52. R. D. Phair, P. Scaffidi, C. Elbi, J. Vecerová, A. Dey, K. Ozato, D. T. Brown, G. Hager, M. Bustin, and T. Misteli, "Global nature of dynamic protein-chromatin interactions *in vivo*: three-dimensional genome scanning and dynamic interaction networks of chromatin proteins," *Mol. Cell. Biol.* **24**, 6393–6402 (2004).
53. A. S. Verkman, "Solute and macromolecule diffusion in cellular aqueous compartments," *TIBS* **27**, 27–33 (2002).